

Synthesis, characterization and applications of polysiloxane networks with immobilized pyrogallol ligands

Salman M. Saadeh¹, Nizam M. El-Ashgar¹, Issa M. El-Nahhal^{2*}, Mohamed M. Chehimi³, Jocelyne Maquet⁴ and Florence Babonneau⁴

¹Department of Chemistry, The Islamic University of Gaza, PO Box 108, Gaza, Palestine

²Department of Chemistry, Al-Azhar University, PO Box 1277, Gaza, Palestine

³ITODYS, Université Paris 7–Denis Diderot, associé au CNRS (UMR 7086), 1 rue Guy de la Brosse, 75005 Paris, France

⁴Laboratoire de Chimie de la Matière Condensée, Université Paris VI, 4 place Jussieu, 75252 Paris, France

Received 8 November 2004; Revised 12 December 2004; Accepted 20 December 2004

A porous, solid insoluble polysiloxane-immobilized ligand system bearing pyrogallol active sites of the general formula $P-(CH_2)_3-NH(CH_2)_3OC_6H_3(OH)_2$ (where P represents $[Si-O]_n$ siloxane network) has been prepared by the reaction of 3-aminopropylpolysiloxane with 1,3-dibromopropane followed by the reaction with pyrogallol. ¹³C CP-MAS NMR and X-ray photoelectron spectroscopy confirmed that the pyrogallol is chemically bonded to the siloxane backbone. Thermal analysis showed that the ligand system is stable under nitrogen at relatively high temperature. The polysiloxane–pyrogallol ligand system exhibits high potential for the uptake of the metal ions (Fe^{3+} , Co^{2+} , Ni^{2+} and Cu^{2+}). Complexation of the pyrogallol ligand system for the metal ions at the optimum conditions was found to be in the order $Fe^{3+} > Cu^{2+} > Ni^{2+} > Co^{2+}$. Copyright © 2005 John Wiley & Sons, Ltd.

KEYWORDS: polysiloxanes; immobilized-polysiloxane ligand systems; propylamine; pyrogallol; metal uptake

INTRODUCTION

Recently, a wide range of applications concerning polysiloxane-immobilized ligand systems^{1–7} have been considered. These organo-modified silicas can be synthesized through the sol–gel process at low temperature. Many ligands have been reported, including thiols,¹ amines,^{1,2} phosphines,³ glycinates,⁴ iminodiacetates,^{5,6} iminodiacetate derivatives⁷ and others.⁸ The polysiloxane-immobilized ligand systems have superior properties over organic resins, owing to their high thermal, hydrolytic, and mechanical stability, in addition to a lack of swelling in solvents.^{9,10} In addition, they exhibit a great potential for extraction, recovery and separation of metal ions from aqueous solution,^{1–7} stationary phases in chromatography⁴ and as supported ligands for catalysts.^{3,11} Characterization of these hybrid systems

has recently been carried out using high-resolution solid-state NMR techniques,^{12,13} as well as other spectroscopic methods.^{14–17}

Pyrogallol was chosen to modify the amino-functionalized ligand system as it introduces the catechol functionality when it condenses with the 3-bromopropyl-*N*-(3-aminopropyl)polysiloxane ligand system. Catechol forms highly stable complexes. For example, enterobactin, a low molecular weight chelating agent produced by bacteria and fungi, coordinates ferric ions octahedrally with six oxygen atoms from three catechol moieties.¹⁸ The resulting molecule has the largest formation constant (approximately 10^{48}) of any known ferric complex.¹⁸

In this study the immobilized pyrogallol ligand system was prepared and characterized using a variety of physical techniques, including high-resolution solid-state ¹³C CP-MAS NMR, X-ray photoelectron spectroscopy (XPS), thermogravimetric analysis (TGA) and Fourier transform infrared (FTIR) spectroscopy. The uptake of metal ions (Fe^{3+} , Co^{2+} , Ni^{2+} and Cu^{2+}) by immobilized pyrogallol ligands was also examined and investigated at different time intervals and pH values.

*Correspondence to: Issa M. El-Nahhal, Department of Chemistry, Al-Azhar University, PO Box 1277, Gaza, Palestine.
E-mail: issaelnahhal@hotmail.com

Contract/grant sponsor: French Ministry of Education, Research and Technology; Contract/grant number: 02-5 0010.

Contract/grant sponsor: Conseil Régional d'Ile-de-France.

EXPERIMENTAL

Reagents and materials

Tetraethylorthosilicate, 3-aminopropyltrimethoxysilane, 1,3-dibromopropane and pyrogallol were purchased from Merck and used as received. Diethyl ether and methanol (spectroscopic grade) were used as received. Metal-ion solutions of the appropriate concentration were prepared by dissolving the metal chloride (analytical grade) in deionized water. The pH range (3.5–6) was controlled by using acetic acid/sodium acetate and pH > 7 by using ammonia/ammonium chloride.

General techniques

Bulk analysis of carbon, hydrogen, and nitrogen were carried out, using an EA 1110-CHNS CE elemental analyzer.

XPS measurements were performed using a Thermo VG ESCALAB 250 instrument equipped with a monochromatic Al K α X-ray source (1486.6 eV, 650 μ m spot size). The samples were mounted onto double-sided adhesive tape. The pass energy was set at 150 eV and 40 eV for the survey and the narrow scans respectively. Additional high-resolution C 1s and N 1s regions were recorded using a pass energy of 10 eV. Charge compensation was achieved with a combination of electron and argon-ion flood guns. The energy and emission current of the electrons were 4 eV and 0.35 mA respectively. For the argon gun, the energy and the emission current were 0 eV and 0.1 mA respectively. The partial pressure for the argon flood gun was 2×10^{-8} mbar. These standard conditions of charge compensation resulted in a negative but perfectly uniform static charge. Data acquisition and processing were achieved with Advantage software, version 1.85. Spectral calibration was determined by setting the main C 1s component due to C–C/C–H bonds at 285 eV. The surface composition was determined using the manufacturer's sensitivity factors. The fractional concentration of a particular element *A* was computed using

$$A(\%) = \frac{I_A/S_A}{\sum(I_n/S_n)} \times 100$$

where I_n and S_n are the integrated peak areas and the sensitivity factors respectively.

^{13}C CP-MAS solid-State NMR experiments were carried out at room temperature on a Bruker AVANCE 300 spectrometer at a frequency of 100.6 MHz. Solid samples were spun at 5 kHz using 7 mm ZrO $_2$ rotors. The contact time was 2 ms, with recycle delays of 5 s. Proton decoupling was applied during acquisition.

Thermogravimetric analysis (TGA) was carried out using Mettler Toledo SW 7.01 analyzer. Additional thermogravimetric/differential scanning calorimetry (TG/DSC) analyses were performed on a SDT2960 TA Instruments equipment under oxygen flow (5 $^{\circ}\text{C min}^{-1}$).

The concentrations of metal ions in their aqueous solutions were measured using a Perkin–Elmer AAnalyst-100 spectrometer.

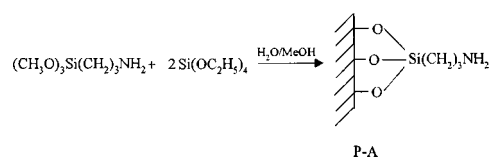
The IR spectra were recorded on a Perkin–Elmer FTIR spectrometer using KBr disks in the range 4000 to 400 cm^{-1} .

All pH measurements were obtained using an HM-40 V pH meter.

Methods of preparation

Preparation of 3-aminopropylpolysiloxane (P–A)

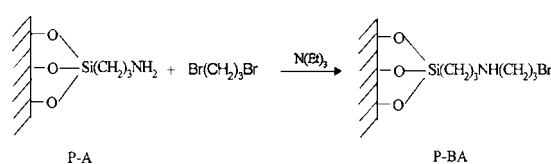
Aminopropylpolysiloxane was prepared as reported previously¹ by adding 3-aminopropyltrimethoxysilane (8.96 g, 0.05 mol) to a stirred solution of tetraethylorthosilicate (20.08 g, 0.1 mol) in a 1 : 2 ratio in the presence of methanol and water (Scheme 1). The product was crushed, sieved, washed with water, methanol and diethyl ether. The material was then dried in a vacuum oven (0.1 Torr) at 90 $^{\circ}\text{C}$ for 10 h.



Scheme 1.

Preparation of 3-bromopropyl-N-(3-aminopropyl) polysiloxane, P–BA

This ligand system was prepared by adding 1,3-dibromopropane in excess (9.0 g, 44.5 mmol) to 3-aminopropylpolysiloxane (5.0 g, 18.5 mmol) in 35 cm^3 of toluene and 2.25 g triethylamine (Scheme 2). The mixture was stirred and refluxed at 110 $^{\circ}\text{C}$ under nitrogen for 48 h. The product was filtered, washed with 0.025 M NaOH, water, ethanol and diethyl ether, and then dried.



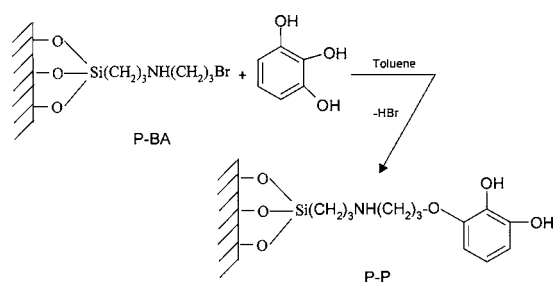
Scheme 2.

Preparation of the immobilized pyrogallol ligand system (P–P)

This ligand was prepared by adding pyrogallol (1.67 g, 13.2 mmol) to a mixture of P–BA in 35 cm^3 toluene and 2.0 g triethylamine (Scheme 3). The mixture was stirred and refluxed at 110 $^{\circ}\text{C}$ under nitrogen for 48 h. The product was filtered and washed with 0.025 M NaOH, water, ethanol and diethyl ether, then dried.

Metal uptake experiments

100 mg of functionalized polysiloxane-immobilized pyrogallol ligand system (P–P) was shaken with 25 cm^3 of a 0.02 M aqueous solution of the appropriate metal ions (Fe^{3+} , Co^{2+} ,



Scheme 3.

Ni^{2+} and Cu^{2+}) using 100 cm³ polyethylene bottles. Determination of the metal-ion concentration was carried out by allowing the insoluble complex to settle and withdrawing an appropriate volume of the supernatant using a micropipette then diluting to the linear range of the calibration curve for each metal. The metal-ion uptake was calculated as millimoles of M^{n+} per gram of ligand. Each study was performed at least in a triplicate. Metal uptake was examined at various pH values.

RESULTS AND DISCUSSION

Elemental analysis

P-A

From the elemental analysis given in Table 1, the percentages of carbon and nitrogen are lower than expected due to the formation of small oligomers leached out during the washing process. The formation of these small oligomers is enhanced by the presence of self-base-catalyzed amino groups; these lead to rapid gelation, so small amounts of non-cross-linked oligomers are formed.¹

P-BA

From Table 1, one can notice lower carbon and larger nitrogen percentages in P-BA than those expected. This is probably due to an incomplete substitution reaction of the amino groups and the 1,3-dibromopropane. Some amino groups may be trapped within the bulk of the polymeric support and, therefore, no longer accessible.^{5,6}

Table 1. Elemental analysis data for P-A, P-BA and P-P

Polysiloxane		C (%)	H (%)	N (%)	C/N
P-A	Expected	15.7	3.9	6.1	3.0
	Found	13.3	4.6	5.2	3.0
P-BA	Expected	18.5	3.3	3.6	5.9
	Found	16.8	4.8	4.3	4.6
P-P	Expected	33.2	4.2	3.2	11.7
	Found	27.6	5.6	3.6	9.2

P-P

As with P-BA, the carbon content is lower than expected and the nitrogen content is larger. This could be due to an incomplete substitution reaction between pyrogallol and the bromide of P-BA.

¹³C CP-MAS NMR spectra

The ¹³C CP-MAS NMR spectra of P-A, P-BA and P-P systems are shown in Fig. 1. The ¹³C CP-MAS NMR spectrum of the P-A (Fig. 1a, Scheme 4) displays three peaks at 9.1 ppm, 20.5 ppm and 41.1 ppm for the three methylene carbon atoms C1, C2 and C3 respectively.¹³ The small peak at 163 ppm could be due to carbonate species adsorbed on ammonium NH_3^+ groups. Indeed, the use of acidic conditions for the preparation of P-A may lead to protonation of the amino groups.

The ¹³C CP-MAS NMR spectrum of the P-BA is given in Fig. 1b (see Scheme 5 for peak assignment). The spectrum shows three signals at 8.8 ppm, 19.8 ppm and 41.7 ppm

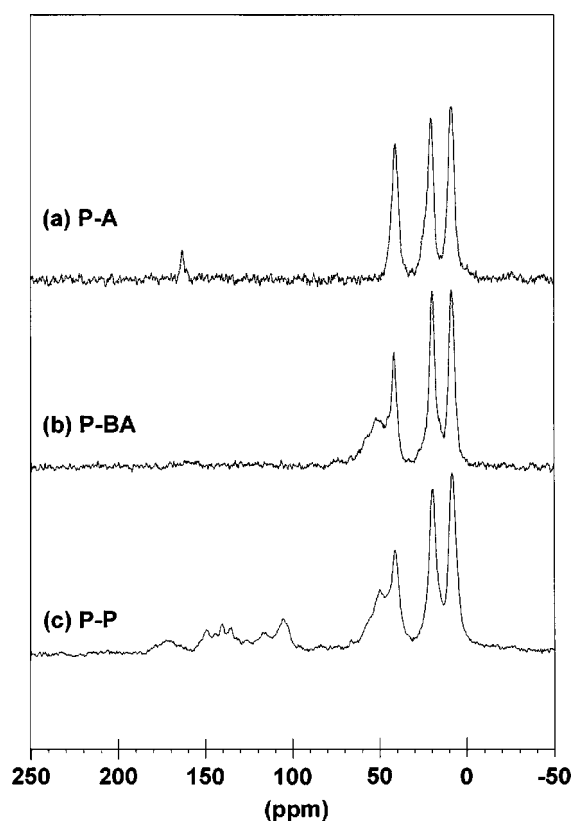
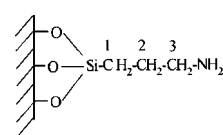
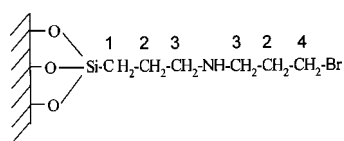


Figure 1. ¹³C CP-MAS NMR: (a) P-A; (b) P-BA; (c) P-P.



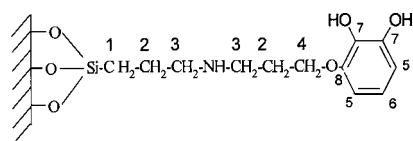
Scheme 4.



Scheme 5.

assigned to the methylene carbon atoms C1, C2, and C3 respectively. The broad signal at 51.9 ppm is assigned to the carbon C4. This broad signal, which is not shown in the ^{13}C NMR for P-A, provides evidence for the introduction of 1,3-dibromopropane from one end.

The ^{13}C CP-MAS NMR spectrum for P-P is given in Fig. 1c (see Scheme 6 for peak assignment). The spectrum shows three carbon signals at 8.6 ppm, 19.7 ppm and 41.3 ppm due to the three methylene carbon atoms C1, C2 and C3 respectively. The broad signal at 50.2 ppm is assigned to carbon atom C4. The spectrum also shows signals at 106 ppm, 116 ppm, 140 ppm and 149 ppm, which are assigned to the aromatic carbon atoms C5, C6, C7 and C8 respectively of the pyrogallol ring. These assignments were based on spectral data taken from literature.^{19–21}



Scheme 6.

XPS

The XPS survey spectra for P-A, P-BA and P-P are shown in Fig. 2. The main peaks are centered at 102.7 eV, 285 eV, 400 eV and 532 eV and correspond to Si 2p, C 1s, N 1s and O 1s core levels respectively.

Br 3d, centered at 68 eV, is visible in the survey scan of P-BA; it is also in that of P-P, indicating that bromine has not been completely removed from this end-polysiloxane even after a thorough washing.

Figure 3 displays the C 1s and N 1s peak fitted spectra for the P-P. The tailed C 1s peak is fitted with six components assigned as follows:²² peak A at 284.8 eV is due to C=C/C-C/C-H (C=C from the pyrogallol group); peak B at 285.8 eV is due to C-N; peak C at 286.6 eV is due to C-O; peak D at 287.9 eV is due to C=O; peak E at 289.4 eV is due to surface ester groups or COO⁻; peak F at 291.5 eV is due to the $\pi \rightarrow \pi^*$ shake-up satellite from the pyrogallol group. The C=O and O-C=O bands are necessary for the fitting and they may be due to a surface contamination of carbonate species adsorbed on the ammonium ion. Actually, an NMR signal due to C=O bonds is also shown in Fig. 1. The N 1s region can be fitted with two main components centered at 399.3 eV (A) and 401.6 eV (B) due respectively to free amine and amine cation/or hydrogen bonding. The free amine

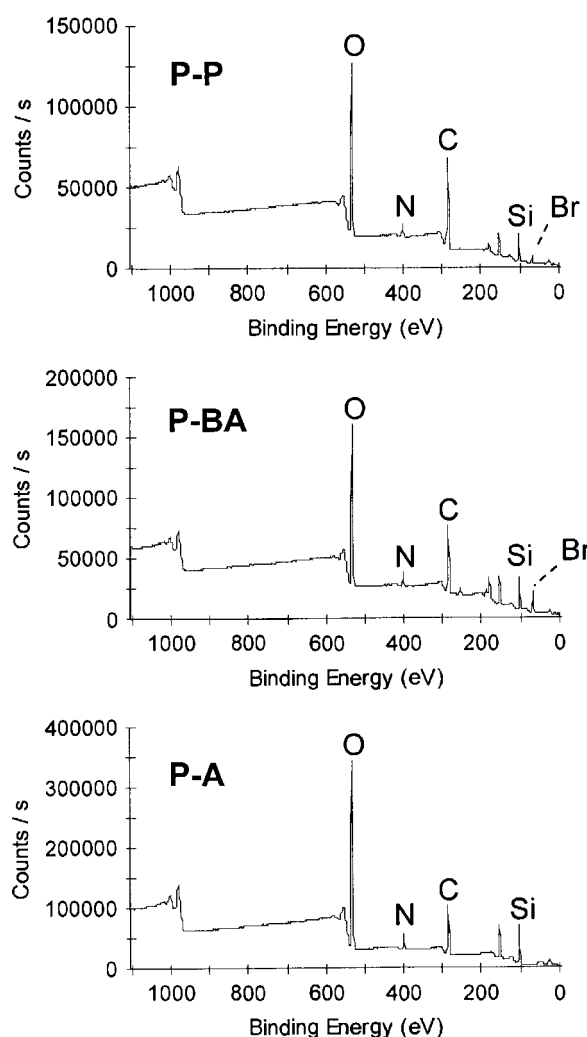


Figure 2. XPS survey spectra of P-A, P-BA and P-P.

proportion is only 47%. Because the component centered at the high binding energy side is wider than that of the free amine, it is likely that the amine undergoes protonation by HCl used in the synthesis or hydrogen bonding with the OH groups from the pyrogallol graft or the silanol groups from the polysiloxane network. The detection of bromine within the P-P network suggests the existence, at least partly, of nitrogen atoms in the form of N^+Br^- .

Table 2 reports the surface composition of the as-prepared and ground polysiloxane systems. There is a slight difference in the surface composition after grinding, but more importantly the C 1s spectra have a much better defined structure and we believe that the spectra obtained after grinding are more convenient for describing the changes in the surface composition of the systems under investigation. It is interesting to note that bromine is detected for the intermediate P-BA material with a surface atomic percent comparable to that of nitrogen therefore accounting for the change in the chemical structure of the aminopropyl ligand.

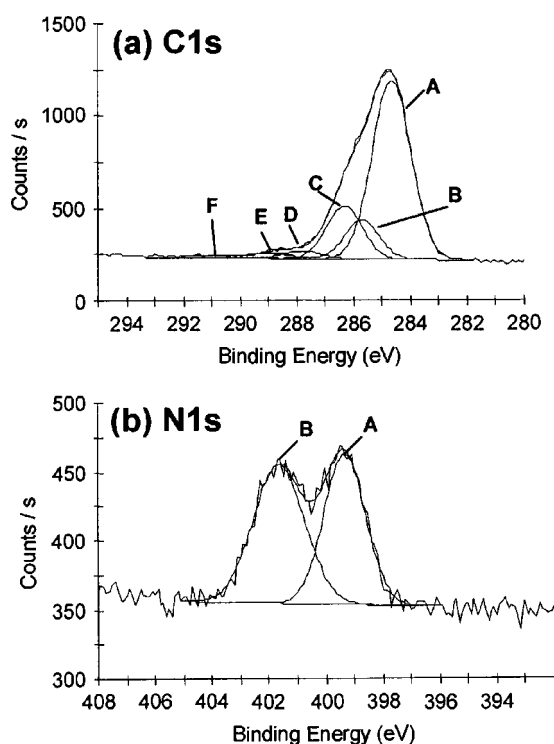


Figure 3. High-resolution C 1s (a) and N 1s (b) regions of P-P.

Table 2. Surface composition of as-prepared and ground polysiloxane-immobilized ligands

Ligand	Analysis (at. %)					
	C	O	Si	N	Br	Cl
P-A	33.8	37.4	24.1	4.45		0.25
P-A ground	28.7	41.0	24.6	5.47		0.29
P-BA	44.4	27.5	18.3	5.35	4.36	
P-BA ground	39.2	31.0	20.5	5.35	3.90	
P-P	47.3	30.6	16.1	4.57	1.38	
P-P ground	47.8	29.8	16.7	4.38	1.38	

Figure 4 shows a plot of the experimental surface C/N ratio versus the theoretical one expected from the structure of the ligands. The C/N ratios for the as-prepared and ground P-P are comparable, whereas for the starting and intermediate materials the C/N ratios are significantly higher before grinding, an indication that P-A and P-BA have a substantial degree of surface contamination. Nevertheless, it is clear that XPS permits the monitoring of the changes in the surface composition that result from the transformation of P-A into P-BA in the first stage and the grafting of the pyrogallol group to P-BA in the second stage that yields P-P.

Thermal analyses

TGA and differential thermogravimetric analysis (DTA) were examined for the polysiloxane-immobilized pyrogallol ligand

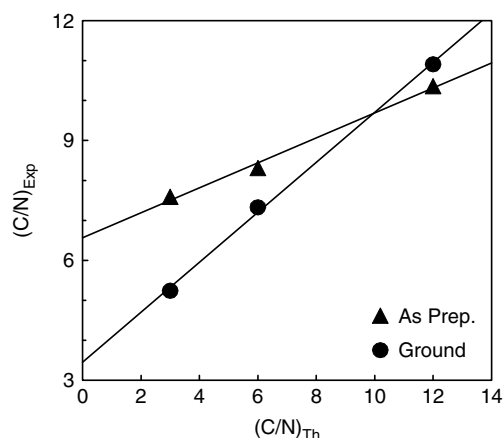


Figure 4. Plots of surface C/N ratio versus the corresponding expected ratio from the structure of the ligands in P-A, P-BA and P-P as prepared (▲) and ground (●).

system (P-P) and its iron complex P-P-Fe(III). The TGA and DTA were performed under nitrogen in the temperature range 20–600 °C. The experiments were performed under nitrogen to avoid oxidation of the pyrogallol and amino groups.

Figure 5 shows the TG curve of P-P. Four peaks are observed in the curve derivative, which have been interpreted by comparison with published data.^{23–25} The first peak occurs at 65 °C, where the ligand system loses 5.8% of its initial weight. This is attributed to loss of physisorbed water and alcohol from the system pores. The second peak, at 250 °C, is due to a further weight loss of 6.0%; this is probably due to dehydroxylation and loss of water from the silica matrix. The third peak, at 350 °C, where the system lost 16.5% of its weight, is attributed to cleavage and degradation of the organofunctional groups bound to silicon atoms. The broad peak between 400 and 600 °C is due to further condensation of hydroxyl groups in the polymer, and which are forming siloxane bonds through dehydroxylation.

The derivative of the TG curve of the P-P-Fe(III) complex (Fig. 6) shows two characteristic peaks at 65 °C and 290 °C and a broad peak in the range 400–600 °C. The second peak is the major peak, in which the complex lost 25% of its initial weight. This is probably due to complex decomposition and degradation of the ligand functional groups.

A simultaneous TG/DSC analysis was performed under oxygen flow on the P-P sample (Fig. 7). A first weight loss of 4.5% occurs before 100 °C and may be due to loss of physisorbed water and alcohol. Above 150 °C, the organic ligands decompose in two steps: between 200 and 400 °C, the 25% weight loss associated with an exothermic peak corresponds to a combustion process; above 400 °C and up to 600 °C, a second weight loss (20%) occurs that is not associated with a strong exothermic peak.

These results show that the P-P sample is moderately stable under an oxidative environment.

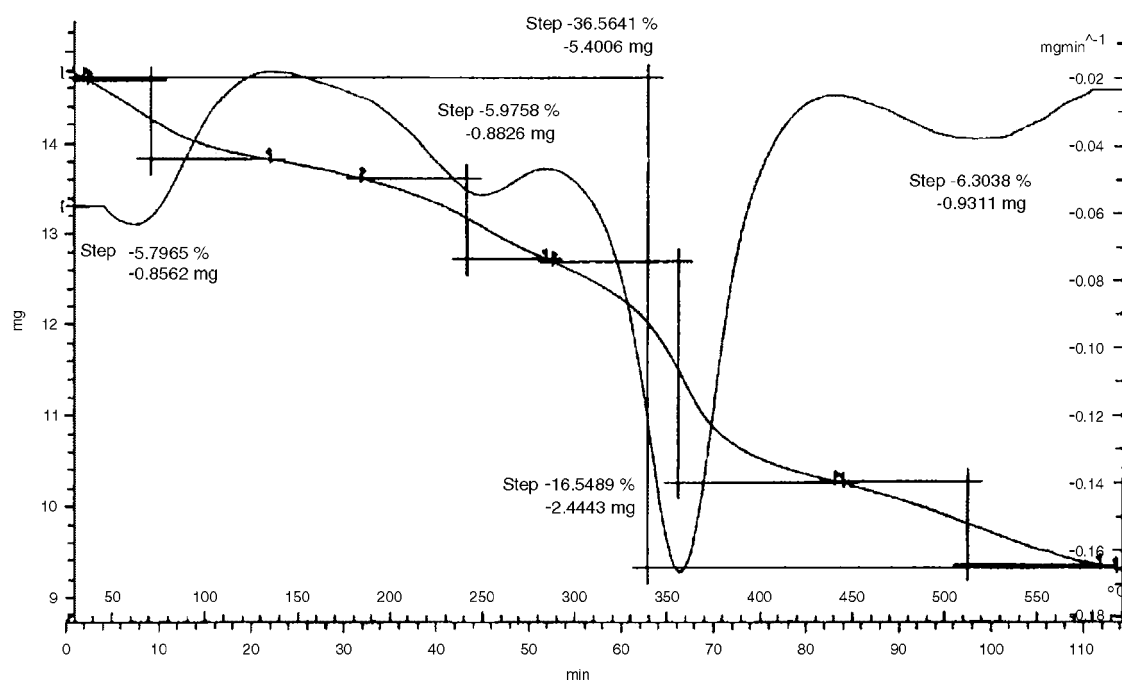


Figure 5. TGA of P-P.

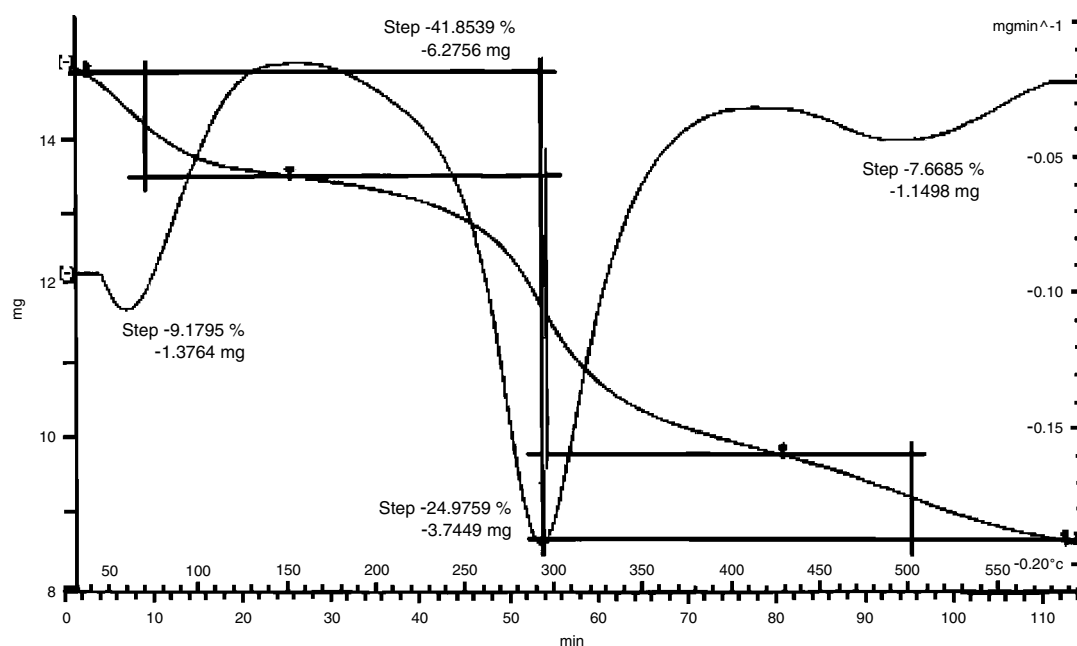


Figure 6. TGA of P-P-Fe(III) complex.

FTIR spectroscopy

The FTIR spectra of P-A and P-P are given in Fig. 8. The two spectra show three characteristic absorption regions: 3500–3000 cm^{-1} due to $\nu(\text{OH})$ or $\nu(\text{NH}_2)$, 1743–1560 cm^{-1} due to $\delta(\text{OH})$ or $\delta(\text{NH}_2)$, and 1200–900 cm^{-1} due to $\nu(\text{Si-O})$. The spectrum of P-P (Fig. 8b) shows strong bands at 3423.7 cm^{-1} and 1628.7 cm^{-1} due to $\nu(\text{OH})$ and $\delta(\text{OH})$ vibrations respectively. This confirms that the pyrogallol

functional group is chemically bonded to the surface of the polysiloxane.

Metal uptake

The metal-ion uptake capacity (Fe^{3+} , Co^{2+} , Ni^{2+} and Cu^{2+}), as mmoles of M^{n+} per gram of ligand, was determined by shaking the functionalized ligand system (P-P) with buffered metal-ion solutions:

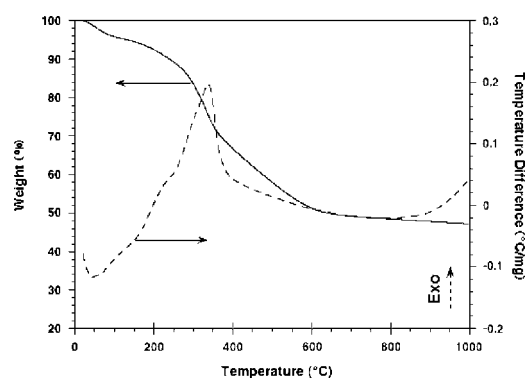


Figure 7. TGA curve (solid line) and DSC curve (dashed line) recorded under oxygen flow on P–P sample.

Metal ion	Fe ³⁺	Co ²⁺	Ni ²⁺	Cu ²⁺
Max. uptake (mmol g ⁻¹)	2.13	1.63	1.74	1.92

The elemental analysis of nitrogen of the immobilized ligand (P–P) was 3.6%, i.e. 2.57 mmol g⁻¹. Comparing this value with the maximum metal-ion uptake, it may be suggested that a 1:1 metal-to-ligand complex is mainly to be expected in the case of Fe³⁺ and Cu²⁺. In the case of Co²⁺ and Ni²⁺ the metal-to-ligand ratio in the complex is smaller than 1:1, indicating that less-stable complexes are formed.

As a whole, the uptake of metal ions decreases in the order Fe³⁺ > Cu²⁺ > Ni²⁺ > Co²⁺.

Effect of shaking time

Measurements of metal-ion uptake by the ligand system P–P were carried out at different time intervals. The uptake of copper ions versus time is given in Fig. 9. It is shown that the metal-ion uptake increases as a function of shaking time and reaches equilibrium after nearly 48 h, where maximum uptake is obtained. Similar results were observed for the other metal ions.

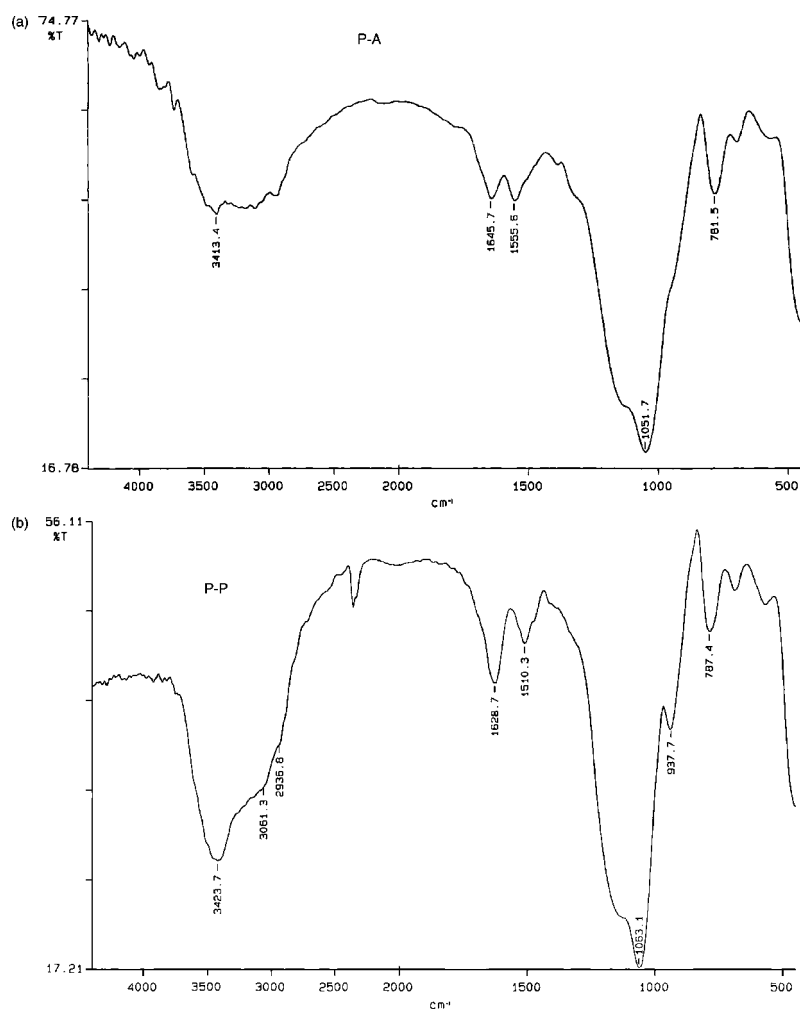


Figure 8. FTIR spectra of (a) P–A and (b) P–P.

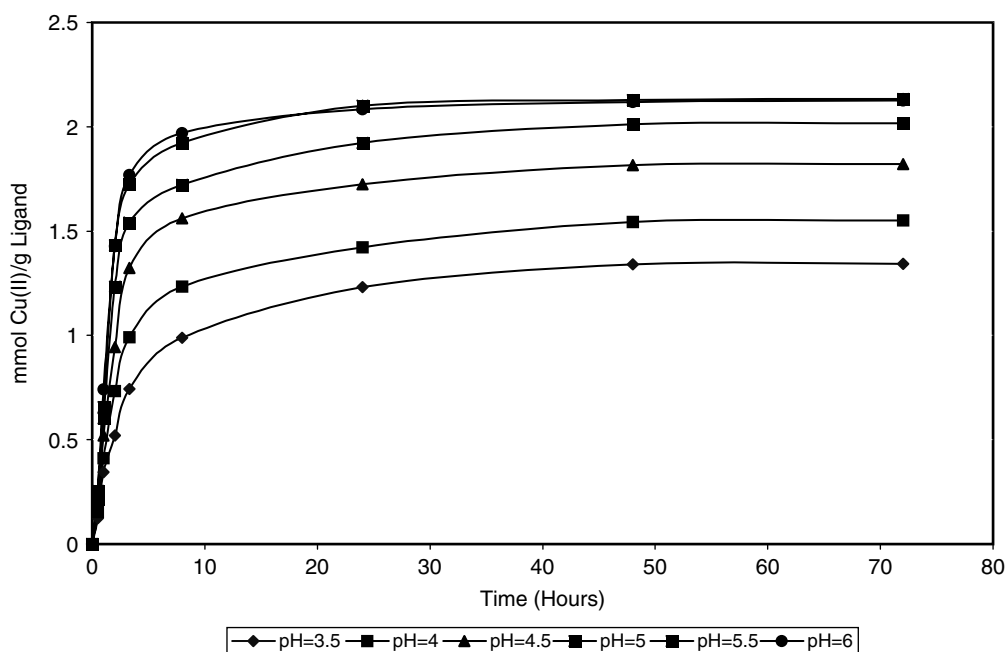


Figure 9. Uptake of Cu^{2+} ions by P-P versus time at pH indicated.

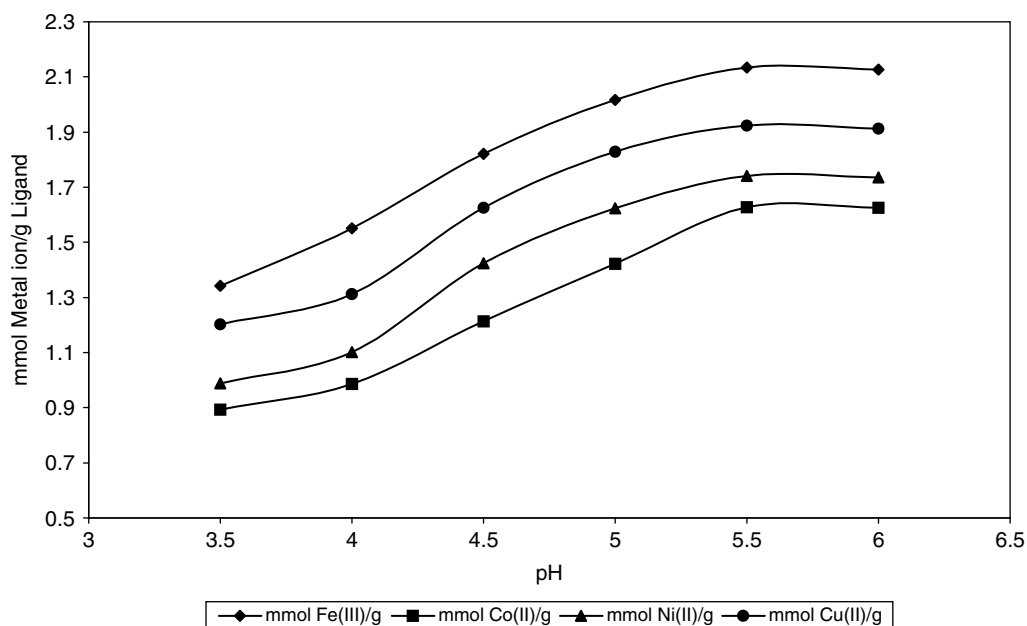


Figure 10. Uptake of metal ions by P-P versus pH (72 h shaking time).

Effect of pH

The effect of the pH value on the uptake of Fe^{3+} , Co^{2+} , Ni^{2+} and Cu^{2+} ions by P-P is shown in Fig. 10. The results show an increase of metal-ion uptake with increasing pH value, reaching a maximum at pH 5.5. Low uptake capacity occurs at lower pH values. This is probably due to the protonation of pyrogallol hydroxyl groups.

CONCLUSIONS

Polysiloxane networks with immobilized pyrogallol ligands have been prepared by reacting aminopropyl-functionalized organosilica (P-A) with first dibromopropane (P-BA) and then pyrogallol (P-P). XPS and ^{13}C MAS-NMR characterization of the polysiloxane-immobilized pyrogallol

system clearly show spectral changes that account for the structural changes of the amino, and then bromoamino groups, into pyrogallol ligands. TGA shows that the pyrogallol ligand system is chemically stable at moderate temperature. This immobilized ligand system exhibits high potential for extraction of some metal ions (Fe^{3+} , Co^{2+} , Ni^{2+} and Cu^{2+}).

Acknowledgements

We wish to thank the French Ministry of Education, Research and Technology for financial support (project no. 02-5 0010) within the framework of a PAI Palestine cooperation. MMC is indebted to the Conseil Régional d'Ile-de-France for financial support through the SESAME 2000 project.

REFERENCES

1. Khatib IS, Parish RV. *J. Organometal. Chem.* 1989; **9**: 369.
2. El-Nahhal IM, Zaggout FR, El-Ashgar NM. *Anal. Lett.* 2000; **33**: 2031.
3. Parish RV, Habibi D, Mohammadi V. *J. Organometal. Chem.* 1989; **369**: 17.
4. El-Nasser AA, Parish RV. *J. Chem. Soc. Dalton Trans.* 1999; 3463.
5. Parish RV, El-Nahhal IM, El-Kurd HM, Baraka RM. *Asian J. Chem.* 1999; **11**: 790.
6. El-Nahhal IM, Zaggout FR, Nassar MA, El-Ashgar NM, Maquet J, Babonneau F, Chehimi MM. *J. Sol-Gel Sci. Technol.* 2003; **28**: 255.
7. El-Nahhal IM, El-Shetary BA, Mustafa AB, El-Ashgar NM, Livage J, Chehimi MM, Roberts A. *Solid State Sci.* 2003; **5**: 1395.
8. Ahmed I, Parish RV. *J. Organometal. Chem.* 1993; **452**: 23.
9. Elfferich FH. *Ion Exchange*. McGraw-Hill: 1962; 26.
10. Lier RT. *The Chemistry of Silica*. Wiley: New York, 1979; 47.
11. Cermak J, Kvicalova M, Blechta V, Capka M, Bastl Z. *J. Organometal. Chem.* 1996; **50**: 77.
12. Yang JJ, El-Nahhal IM, Chung IS, Maciel GE. *J. Non-Cryst. Solids* 1997; **209**: 19.
13. Yang JJ, El-Nahhal IM, Maciel GE. *J. Non-Cryst. Solids* 1996; **204**: 105.
14. Chiang CH, Ishida H, Koenig JL. *J. Colloid Interface Sci.* 1980; **74**: 396.
15. Ishida H, Chiang CH, Koenig JL. *Polymer* 1982; **23**: 251.
16. Taylor I, Howard AG. *Anal. Chim. Acta* 1993; **271**: 77.
17. El-Nahhal IM, Chehimi MM, Cordier C, Dodin G. *J. Non-Cryst. Solids* 2000; **275**: 142.
18. Harris WR, Carrano CJ, Cooper SR, Sofen SR, Avdeef A, McArdle JV, Rymond KN. *J. Am. Chem. Soc.* 1979; **101**: 6097.
19. Maciel GE, Chuang I, Gollob L. *Macromolecules* 1984; **17**: 1081.
20. Amram B, Laval F. *J. Appl. Polym. Sci.* 1989; **37**: 1.
21. Wawer I, Zielinska A. *Solid State Nucl. Magn. Reson.* 1997; **10**: 33.
22. Beamson G, Briggs D (eds). *High Resolution XPS of Organic Polymers, The Scienta ESCA306 Data Base*. John Wiley: Chichester, 1992.
23. Klonkowski AM, Koehler K, Schlaepfer CW. *J. Mater. Chem.* 1993; **3**: 105.
24. Klonkowski AM, Widernik T, Grobelna B. *J. Sol-Gel Sci. Technol.* 2001; **20**: 161.
25. Jovanovic JD, Govedarica MN, Dvornic PR, Popovic IG. *Polym. Degrad. Stabil.* 1998; **61**: 87.